ISSN 1330-3651 (Print), ISSN 1848-6339 (Online)
https://doi.org/10.17559/TV-20230426000572
Original scientific paper

Analysis of Power Losses in Constrained Cycloid Drive

Tihomir MAČKIĆ, Nenad MARJANOVIĆ, Milan TICA*, Sanjin TROHA, Miroslav MILUTINOVIĆ, Nebojša RAŠOVIĆ

Abstract: The aim of this paper is to present a theoretical model for efficiency evaluation of a simple cycloid drive train with one degree of freedom (DOF) or constrained cycloid drive. In order to evaluate the efficiency, it is necessary to find the losses generated in the simple cycloid drive, where only losses depending on the load were considered. Expressions for determining speed ratios, efficiency, velocities and forces acting inside the cycloid drive are presented. These expressions are implemented in the theoretical model, where the places where the losses occur are defined. A computer program was created to facilitate analysis and obtain loss values based on different input data. Only load-dependent losses were considered in the theoretical model and computer program. In order to verify the theoretical model, experimental measurements were performed. A physical model of the simple cycloid drive train was created and analyzed on the test bench. The results for "*S1*" operating mode, i.e. when shaft 2 is stopped, show a mean value of the efficiency of 63.49%, for experimental measurements, while the mean value for theoretical analysis is 65.25%. For the operating mode "*S2*", i.e. with shaft 1 stopped, the mean value of the experimental measurements of the efficiency is 60.9%, while the theoretical mean value is 62.82%.

Keywords: constrained cycloid drive; cycloid drive; efficiency; losses

1 INTRODUCTION

Gears with a cycloid profile or cycloid gears have found their application in many modern drive trains, which require compactness, a large speed ratio, reliable operation, and a high efficiency. The drive trains that use cycloid gears or shorter cycloid drive train are mostly planetary transmissions and today they are often used as a single-stage cycloid drive train with one degree of freedom [1, 2], which can be called constrained cycloid drive. Fig. 1 shows a schematic view of the simple cycloid drive train, which consists of the following basic members [3]: central ring with rollers (*1*), cycloid gear (*1p*), disc with rollers (*2*) and carrier or eccentric shaft (*S*).

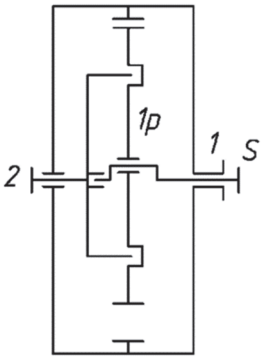

Figure 1 Simple cycloid drive train [3]

Determining the efficiency of a cycloid drive train is a very complex problem and is insufficiently investigated today. In the manufacturer's catalogs [1, 2], the efficiency is given as a constant value, regardless of the different speed ratio and other characteristics of the cycloid drive trains.

The first significant research on the efficiency of cycloid drive was done by Malhotra and Parameswaran, where they assumed the ideal geometry of the cycloid gears and that the value of the normal force is proportional to the distance from the kinematic pole [4]. Measurement of the efficiency under static load was done by Kosse [5] by measuring the area of the hysteresis loop, in which he established the efficiency of less than 65%, with the fact that for complex drive trains it can be even below 20%. This efficiency is much lower compared to the efficiency under dynamic load, so it is not relevant for operating conditions. Gorla et al. [6] presented an innovative design of a cycloid drive train, where the central ring is made with cycloid teeth. When analyzing the distribution of contact forces, they assumed that the elements are absolutely rigid, with ideal geometry and without friction. The authors calculated the efficiency by taking into account all partial power losses. Analytical expressions for calculating partial losses were obtained through kinematic analysis and simplified calculation for forces. They confirmed the accuracy of the analytical expressions experimentally on the cycloid drive model, where they changed the working conditions, i.e. angular velocity and torque.

The contact forces between the meshing elements are very important for obtaining more precise values of friction forces, which influence the overall efficiency. At first, analytical expressions were used, which assumed an ideal load distribution [7, 8], while later numerical calculations were developed [9-12]. The distribution of contact forces and stresses is highly dependent on the clearances and tolerances between the meshing parts. Sensinger [13] presented a unified set of equations for calculating forces, efficiency and moment of inertia, including the clearances and profile corrections. He et al. [14] gave an overview of previous research that takes into account the influence of tooth profile modifications (TPMs) of the cycloid gear on the performance of cycloid drive. The paper presents a quasi-static load distribution model, with consideration of 4 types of profile modification.

There is considerable research and analysis of gerotor or trochoidal pump efficiency [15-19]. These studies can, with appropriate modifications, also be applied to cycloid drives. Sensinger [20], using the theoretical method given in [21] and with experimental measurements, established the difference in the efficiency between a single-stage and a reduced two-stage cycloid drive, with the same speed ratios. In addition, he compared the difference in the efficiency if fixed or free (rolling) pins were placed in the central ring. Blagojević et al. [22] presented the calculation of cycloid drive friction forces for four different values of the friction coefficient. The paper [23] analyzed the influence of geometric and kinematic parameters on the

efficiency of the cycloid drive, where the coefficient of friction was considered constant.

In addition to the classic cycloid drive, modified variants and prototypes of drives were also investigated. In papers [24-26], dynamic analysis and optimization of the shape of meshing elements were performed, while in paper [27] the efficiency of a novel planar ball reducer based on a rolling bearing was examined.

In the case of a simple cycloid drive train, the biggest influence is the loss of power due to friction between the teeth of the cycloid gear and the central ring rollers [5, 6]. These power losses are directly and indirectly influenced by various geometric, kinematic and other parameters, where the contact forces, as well as the sliding and rolling speeds between the contact surfaces, are the most important [13, 23]. Therefore, in this paper, only load-dependent losses will be analyzed.

2 SPEED RATIOS AND VELOCITIES

In papers [28, 29], it is defined the *basic speed ratio*, as:

$$i_0 = \left(\frac{n_1}{n_2}\right)_{n_s=0} \tag{1}$$

where is: n_1 - speed of central ring shaft *1*, n_2 - speed of disc shaft *2*, n_s - speed of eccentric shaft *S*.

Tab. 1 shows the expressions for the speed ratios of constrained cycloid drive, when it is assumed that the number of rollers is one greater than the number of teeth.

Table 1 The equations of speed ratio of constrained cycloid drive [28]

Description	The equations of speed ratio	
Minimum multiplication	$i_{12} = i_0$	$i_{12} = z_1 - 1/z_1$
Minimum reduction	$i_{21} = 1/i_0$	$i_{21} = z_1/z_1 - 1$
Maximum multiplication	$i_{1S} = 1 - i_0$	$i_{1S} = 1/z_1$
Maximum reduction	$i_{S1} = 1/1 - i_0$	$i_{S1} = -z_1$
Reversible multiplication	$i_{2S} = 1 - 1/i_0$	$i_{2S} = 1/1 - z_1$
Reversible reduction	$i_{S2} = i_0/i_0 - 1$	$i_{S2} = 1 - z_1$

The velocities and kinematic gearing model of simple cycloid drive are similar to the kinematic model of trochoid pump. The research presented in references [15-17] can be used to define a kinematic model of cycloid drive.

The absolute velocity of the profile of the central ring and cycloid gear (Fig. 2), at the point of contact *P*, is respectively [15, 16]:

$$\begin{aligned} v_t &= v = v_{pt} + v_{rt} \\ v_a &= v = v_{pa} + v_{ra} \end{aligned} \tag{2}$$

where the index *p* corresponds to the transfer and the index *r* to the relative velocity.

The summary rolling velocity is [16, 17]:

$$v_\Sigma = \left\{ ez_1 \left(1 + \lambda^2 + 2\lambda\cos\beta\right)^{\frac{1}{2}} - r_c \left(1 + 2\delta'\right) \right\} \omega_r \tag{3}$$

$$\delta' = \frac{(z_1 - 1)\left[1 - \lambda\cos\beta\right]}{1 + \lambda^2 - 2\lambda\cos\beta} \tag{4}$$

$$\omega_r = \left|\omega_t - \omega_a\right| = \left|\omega_t - \frac{Z_1 - 1}{Z_1}\omega_t\right| = \left|\frac{\omega_t}{Z}\right| \tag{5}$$

where is: e - eccentricity, λ - coefficient of the trochoid [15], r_c - outer radius of the rollers on central ring, β - rotation angle of cycloid gear, ω_t - angular velocity of cycloid gear, ω_a - angular velocity of central ring.

The intensities of the relative velocities of the meshing profiles at the point of contact are determined by the following equations:

$$v_{rt} = \left\{ ez_1 \left(1 + \lambda^2 + 2\lambda\cos\beta\right)^{\frac{1}{2}} - r_c \left(1 + \delta'\right) \right\} \omega_r \tag{6}$$

$$v_{ra} = r_c \delta' \omega_r \tag{7}$$

The sliding velocity at the point *P*, which increases wear and the possibility of pitting, occurs only if there are fixed pins around on the central ring and can be eliminated by placing rollers or bearings on the central ring pins (Fig. 3). In this way, sliding and wear are no longer present at point *P*, since the bearing rotates freely around point *D*. At the same time, the peripheral velocity of the outer ring of the bearing is equal to the relative velocity of the cycloid gear profile at the meshing point *P*. Then at the point *P*, only rolling is present, without sliding. If the coordinate system Dx_dy_d is fixed at point *D*, then the angular velocity of the roller, in relation to the coordinate system Dx_dy_d, will be:

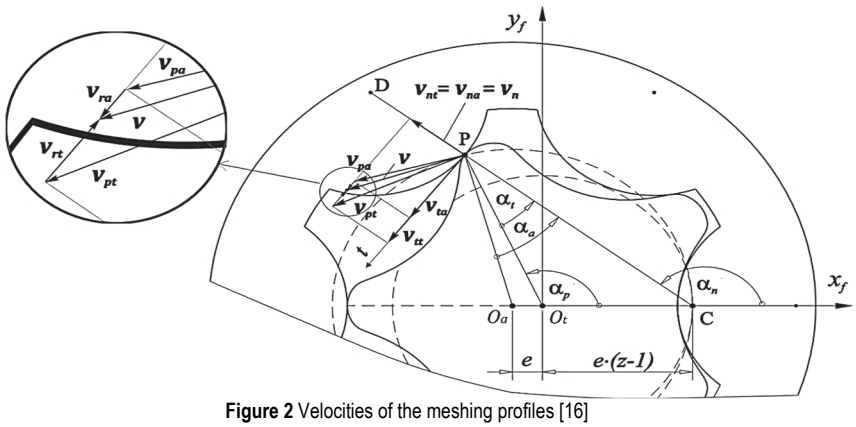

Figure 2 Velocities of the meshing profiles [16]

$$\omega_{rt1} = \frac{2}{d_{v1}}|v_{rt}| \tag{8}$$

where is: d_{v1} - outer diameter of the roller.

The sliding is transferred to the contact point T (Fig. 3), between the roller, which rotates around the point D, and the pin. Thus, the sliding velocity of the pin relative to the coordinate system Dx_dy_d is equal to:

$$v_{r1} = |v_{rt1} - v_{ra1}| = \frac{d_{o1}}{d_{v1}}|v_{rt} - v_{ra}| = \frac{d_{o1}}{d_{v1}}v_r \tag{9}$$

where is: d_o - inner diameter of the roller.

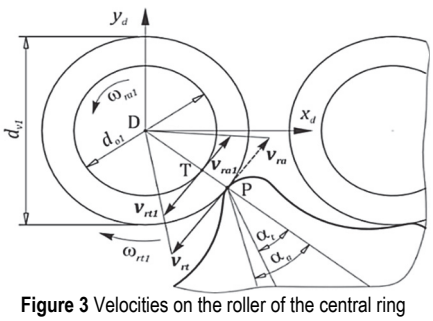

Figure 3 Velocities on the roller of the central ring

3 FORCES AND TORQUES

Fig. 4 shows the forces and torques acting on the cycloid gear. Exactly the same forces act on the second cycloid gear, which is rotated by 180°. Further analysis of the parameters will be performed only for one cycloid gear.

The torques acting on the cycloid gear are:

- Torque on the central ring T_1.
- Torque on the disc T_1.
- Torque on eccentric shaft T_S.

From Fig. 4, the following forces can be observed:

- F_N - normal force, between the tooth of the cycloid gear and the central ring roller.
- F_K - normal force between the cycloid gear and the disc roller.
- F_E - force on eccentric shaft

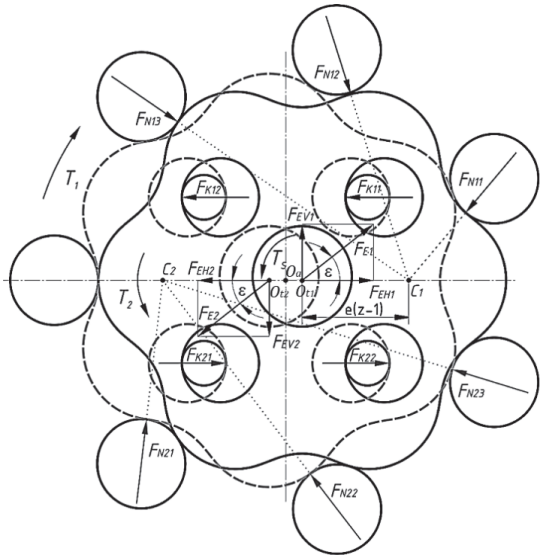

Figure 4 Forces and torques acting on cycloid disc

1) Normal force F_N (Fig. 5):

If the central ring turns by an angle $\Delta\varphi$, then the displacement in the normal direction at the meshing point will be:

$$\Delta l_N = \Delta l \sin\delta_c = r\Delta\varphi\sin\delta_c \tag{10}$$

The force in the normal direction is equal to:

$$F_N = c_N \Delta l_N = c_N r \Delta\varphi \sin\delta_c \tag{11}$$

where is: c_N - stiffness between meshing elements.

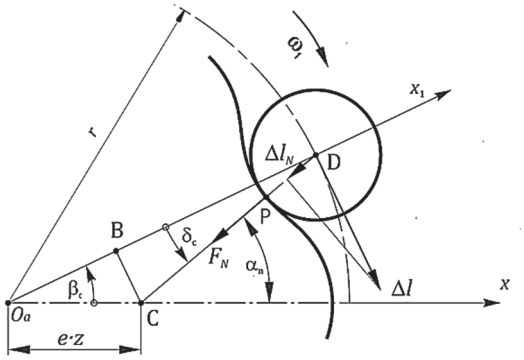

Figure 5 Force on central ring roller [30]

In order to find the values of force F_N, it is necessary to determine the product $k_{N1} = c_N r\Delta\varphi$, which is obtained by an iterative procedure, using the equation [17, 30]:

$$T_1 = k_{N1}\sum_i ez\sin\delta_{ci}\sin\alpha_{ni} \tag{12}$$

where is: δ_{ci} - grip angle on i-th roller, α_{ni} - the angle between the x-axis and the line that passes through the points C and P.

2) Normal force F_K (Fig. 6):

If the disc is turned by an angle $\Delta\varphi$, then the displacement in the direction of the normal at the meshing point will be:

$$\Delta l_{Kj} = \Delta l_j \sin\left(\alpha_{Kj} + \beta_{c2}\right) = r_{m2}\Delta\varphi\sin\left(\alpha_{Kj} + \beta_{c2}\right) \tag{13}$$

where is: r_{m2} - pitch radius of disc rollers, α_{Kj} - straight line which connects the point O_a with the center of the j-th disc roller, β_{c2} - the rotation angle of the disc and is calculated as:

$$\beta_{c2} = \beta_c \frac{z_1}{z_1 - 1} \tag{14}$$

The value of the force F_K on the j-th disc roller can be obtained using the expression:

$$F_{Kj} = c_K \Delta l_{Kj} = c_K \Delta\varphi r_{m2}\sin\left(\alpha_{Kj} + \beta_{c2}\right) \tag{15}$$

where is: c_K - stiffness between meshing elements.

The product $c_K\ \Delta\varphi$ is obtained by an iterative procedure, using the equation:

$$T_2 = c_K \Delta\varphi \sum_j \left[r_{m2} \sin\left(\alpha_{Kj} + \beta_{c2}\right) \right]^2 \tag{16}$$

3) Force on eccentric shaft F_E (Fig. 4):
Vertical component:

$$F_{EV} = \sum_j F_{Ni} \sin\alpha_{Ni} \tag{17}$$

Horizontal component:

$$F_{EH} = \sum_i F_{Ni} \cos\alpha_{Ni} + \sum_j F_{Kj} \tag{18}$$

The force F_{EV} can also be found using the expression:

$$F_{EV} = \frac{T_s}{e} \tag{19}$$

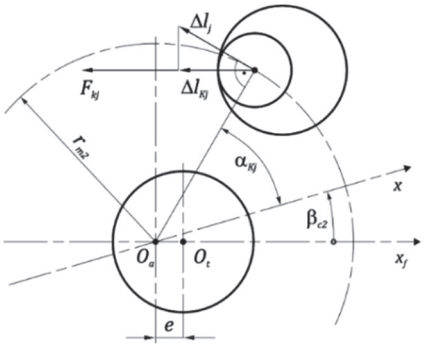

Figure 6 Force on disc roller

4 LOSSES AND EFFICIENCY

Defining the expression for determining the efficiency of the cycloid drive is done by determining the total power losses or calculating the total work of the friction forces [4, 6]. In this paper, analytical expressions for power losses are developed based on kinematic analysis and simplified force calculations. In order to determine the power losses in the simple cycloid drive, the so-called basic mode will be observed, where the carrier or eccentric shaft is stopped $\omega_s = 0$ or considered stopped. The total power losses can be divided by segments and given by the following expressions:

A) Losses in the bearing between cycloid gear and eccentric shaft:

The determination of the power losses in the bearing can be simplified based on the following expression:

$$P_{L1} = M_a \left|\omega_v - \omega_u\right| = \mu_{r1} F_E \frac{D_p}{2} \left|\omega_v - \omega_u\right| \tag{20}$$

where is: D_p - outer diameter of bearing, μ_{r1} - coefficient of friction of bearing, ω_v - angular velocity of the outer ring of bearing, ω_u - angular velocity of the inner ring of bearing.

Since the eccentric shaft is considered to be stopped, when only relative power is transmitted, it can be written:

$$P_{L1} = \mu_{r1} \frac{D_p}{2} \frac{1}{i_o} \left|\omega_1 - \omega_S\right| \sqrt{{F_{EV}}^2 + {F_{EH}}^2} \tag{21}$$

B) Losses between the disc roller and the hole of cycloid gear:

The assumption is that one uses plain or needle bearings, placed on the pins, so in this case only the rolling of the bearings occurs. The rolling speed of the bearings is equal to:

$$v_{r2} = \frac{1}{2} D_{CZ} \left|\omega_p - \omega_S\right| \tag{22}$$

where is: D_{CZ} - diameter of hole, ω_p - angular velocity of cycloid gear.

Therefore, the power losses are:

$$P_{L2} = v_{r2} \sum_j \mu_{r2}(j) F_{kj} \tag{23}$$

where is: $\mu_{r2}(j)$ - coefficient of rolling friction between the j-th roller and the hole.

C) Losses between the rollers and the pins of the disc:

Slippage occurs between the roller and the disc pin. The sliding speed, in relation to the fixed coordinate system related to the central axis, is:

$$v_{s3} = \frac{D_{CZ}}{2} \frac{d_{o2}}{d_{v2}} \left|\omega_p - \omega_S\right| \tag{24}$$

where is: d_{o2} - diameter of disc pin, d_{v2} - outer diameter of disc roller or bearings.

The power losses are:

$$P_{L3} = v_{r3} \sum_j \mu_{s3}(j) F_{kj} \tag{25}$$

where is: $\mu_{s3}(j)$ - coefficient of sliding friction between the j-th roller and pin.

D) Losses between the cycloid gear and the central ring rollers:

At the meshing point, rolling occurs and the rolling speed is equal to the relative speed of the cycloid gear profile, Eq. (6), so the losses due to rolling friction are:

$$P_{L5} = \sum_i \mu_{r5}(i) F_{Ni} v_{rt}(i) \tag{26}$$

where is: $\mu_{r5}(i)$ - coefficient of rolling friction between the i-th roller and cycloid disc, $v_{rt}(i)$ - relative velocities of cycloid disc profile at the meshing point on the$i$-th roller.

E) Losses between the rollers and the pins of the central ring:

It is assumed that these losses, in addition to the losses between the rollers and the pins of the disc, affect the total losses the most. Inserting the Eq. (9), the power losses can be obtained as:

$$P_{L6} = \frac{d_{o1}}{d_{v1}} \sum_i \mu_{s6}(i) F_{Ni} \left| v_r(i) \right| \tag{27}$$

where is: $\mu_{s6}(i)$ - coefficient of sliding friction between the *i*-th roller and pin, $v_r(i)$ - sliding velocities at the meshing point on the *i*-th roller.

Total power losses are calculated as the sum of partial losses, so the total efficiency can be written in the form:

$$\eta = \frac{P_{ul} - P_L}{P_{ul}} = 1 - \frac{1}{P_{ul}} \sum_{i=1}^{n} P_{L_i} = 1 - \sum_{i=1}^{n} \varsigma_i = 1 - \varsigma \tag{28}$$

where is: P_{ul} - input power, ς_i - partial power loss factors, ς -total power loss factor.

If needle bearings are used as rollers, the SKF model [31] will be used for power loss calculations, where only load-dependent losses will be taken into account. The values of the instantaneous friction coefficients were obtained based on the methods and results given in the paper [16].

The efficiency from Eq. (28) is same as the basic efficiency, which is explained in paper [3] and is given as:

$$\eta_o = \eta_{12} = -\left(\frac{T_2 \omega_2}{T_1 \omega_1} \right)_{\omega_s = 0} \tag{29}$$

The expressions for the other efficiencies (Tab. 2) can be obtained, applying the method from paper [3]. The sequence of indices symbolizes the input and output shaft, respectively, without the symbol of the stopped shaft.

Table 2 The equations of efficiency of constrained cycloid drive

	η_{12}	η_{21}	η_{1S}	η_{S1}	η_{2S}	η_{S2}
w	+1	−1	−1	+1	−1	+1
$f(\eta_O, i_O)$	η_O	η_O	$\frac{\frac{i_o}{\eta_o} - 1}{i_o - 1}$	$\frac{i_o - \eta_o}{i_o \eta_o - 1}$	$\frac{i_o - \eta_o}{i_o - 1}$	$\frac{i_o - 1}{i_o - \frac{1}{\eta_o}}$

Using the derived Eq. (20) to Eq. (28), it is possible to obtain values of partials and total loss. In order to obtain the value of losses more easily, a computer program was developed in the Matlab software package. Fig. 7 shows the calculated value and impact of individual power losses.

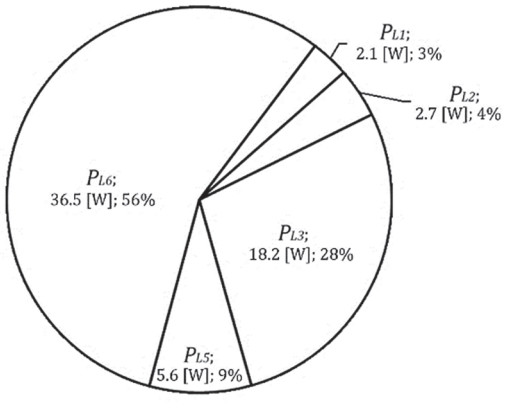

Figure 7 Partial losses

5 EXPERIMENTAL RESULTS AND COMPARISON

Fig. 8 shows the tested model of simple cycloid drive, which consists of basic elements: 1 - disc, 2 - central ring, 3 - eccentric shaft and 4 - cycloid gear.

The gear and shaft material is C45 steel, which has been further improved to a hardness of 40 HRC. Roller bearings were used, instead of sliding bearings, in order to obtain better efficiency. Lithium-complex grease NLGI class 2 (standard DIN 51502, KP2PN-20) with kinematic viscosity ν_k = 200 mm^2/s was used for lubrication.

Finish quality was measured using a Mitutoyo surftest SJ-310 roughness meter. On the profile of the teeth, the mean roughness value of 1.221 μm was measured, while the mean roughness value of 0.953 μm was obtained in the holes of the cycloid gear. The mean value of the roughness of the outer rings of the needle bearings was also measured, which is 0.763 μm.The average value of bearing and profile roughness is calculated as:

$$R_a = \sqrt{R_{a1}^2 + R_{a2}^2} \tag{30}$$

where is: R_{a1}, R_{a2} - roughness of individual surfaces, μm.

The measurements and corrections presented in paper [30] were implemented and entered into the software, in order to obtain the most accurate values of the contact forces. The gear is made with a profile correction of δ_{rz} = 0.05 mm, which ensures the necessary clearance during meshing.

Test bench was constructed and made, which is located in the Laboratory for Measuring Techniques, at the Faculty of Mechanical Engineering in Banja Luka (Fig. 9). The test bench enables the measurement of revolutions and torques on transmission shafts and consists of: 1 - frequency regulator, 2 - electric motor with nominal power P = 250 W and revolutions n = 2800 rpm, 3 - optical speed sensor HySense RS110, 4 - torque transducer HBM T22/20, 5 - tested simple cycloid drive train, 6 - torque and speed transducer HBM T30FN, 7 - mechanical brakes with felt.

Table 3 Input data

Symbol	Data	Value
e	Eccentricity / mm	2
λ	Coefficient of the trochoid	1.6
d_{v1}	The diameter of the rollers on the central ring / mm	12
d_{v2}	The diameter of the rollers on the disc / mm	14
z_1	Number of rollers on the central ring	15
k	Number of rollers on the disc	7
i_o	Basic speed ratio	14/15
δ_{rz}	The size of the profile correction / mm	0.05
b_1	The width of rollers on the central ring / mm	12
b_2	The width of rollers on the disc / mm	12
d_{m2}	Pitch diameter of the disc rollers / mm	56
D_p	Outer diameter of cycloid gear bearing / mm	32
ν_k	Kinematic viscosity of grease / mm^2/s	200
R_{a1}	Mean roughness of cycloid gear teeth / μm	1.263
R_{a2}	Mean roughness of cycloid gear holes / μm	1.439

All transducers and sensors are connected to the HBM QuantumX MX840A data acquisition device, which is

connected to the HBM catman®Easy data visualization and analysis program. This enables the simultaneous measurement and analysis of input and output data and obtaining the value of the efficiency in real time.

In order to compare the mathematical with the physical model, it is necessary to enter all the known data into the computer program for the calculation of losses. These data are presented in Tab. 3. Only the reduction modes of operation, i.e. with stopped shaft *1* or *2*, where the input eccentric is shaft *S*, were tested

a) Physical model

b) Disassembled cycloid drive

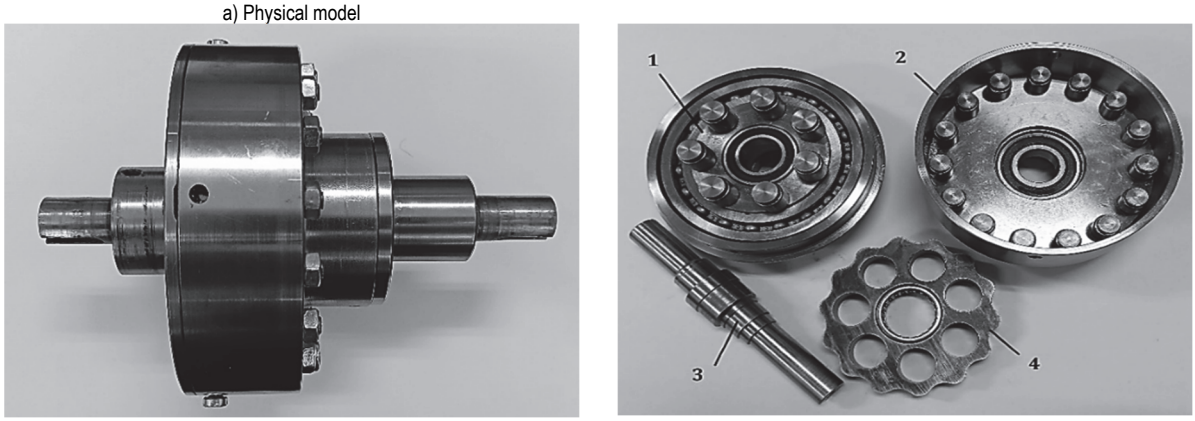

Figure 8 Experimentally tested simple cycloid drive

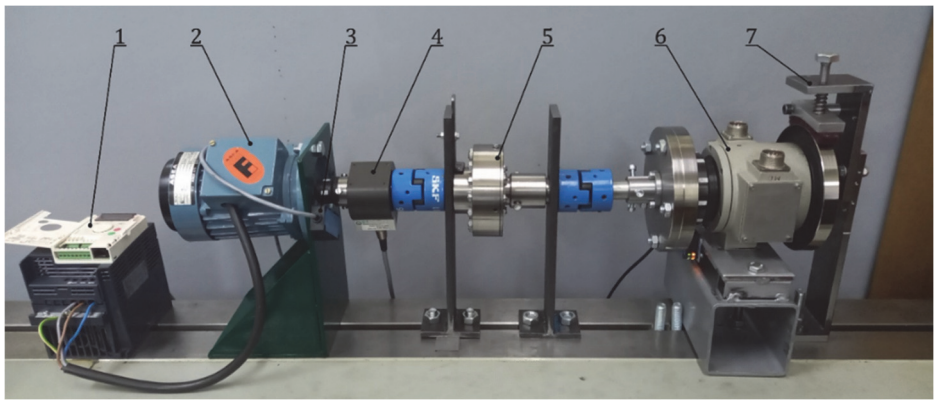

Figure 9 Test bench

Fig. 10 shows the results of the theoretical and experimental analysis in the "*S*1" operating mode, i.e. when the input shaft is *S* (eccentric shaft) and the output shaft is *1* (central ring shaft), with the shaft *2* stopped.

The left graph shows the results of the efficiency depending on input torque and speed, while the ratio of input and output power is shown on the right side (Fig. 10b). An increase in efficiency can be observed with increasing torque values. In addition, the larger deviations of the experimental and theoretical results are at lower input power values.

In experimental tests, the efficiency varies from 61.50% to 64.85%, while the average value is 63.49%. In the case of theoretical results, the efficiency ranges from 63.75% to 66.12%, while the average value is 65.25%. The assumption is that the difference between theoretical and experimental results, for output power, is a consequence of losses that were not considered in the theoretical analysis. Therefore, these losses will be calculated through the factor of additional power losses, as:

$$\varsigma_d = \frac{P_t - P_e}{P_{ul(e)}}, \% \tag{31}$$

where is: P_t - theoretical result of output power, P_e - experimental result of output power, $P_{ul(e)}$ - experimentally measured input power.

In order to evaluate the accuracy of theoretical results, the mean value of the factor of additional power losses will be taken into account, which is 1.76%, for the simple cycloid drive in the "*S*1" operating mode.

Fig. 11 shows the results of the theoretical and experimental analysis in the "*S*2" operating mode, i.e. when the input is eccentric shaft *S* and the output is disc shaft *2*, with the central ring shaft *1* stopped.

The efficiency varies, for experimental tests, from 58.21% to 63%, while the average value is 60.9%. In the case of theoretical results, the efficiency ranges from 61% to 63.99%, while the average value is 62.82%. The mean value of the additional loss factor is 1.92%.

The same as for the "*S*1" operating mode, there is a much better matching between the results of the theoretical and experimental analysis at higher values of the input power. Better efficiency is obtained when the central ring shaft *1* is the output shaft, which correlates with the results from paper [3], for cycloid drive with stepped cycloid gear. Similar results of efficiency change were obtained in the experimental results presented in paper [32], where a classic cycloid drive with two cycloid gears was investigated.

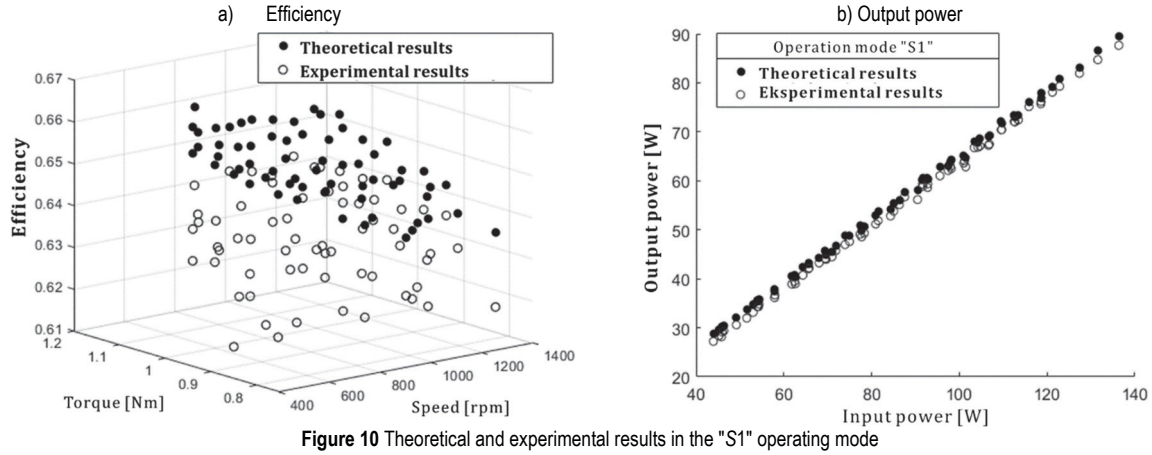

Figure 10 Theoretical and experimental results in the "*S*1" operating mode

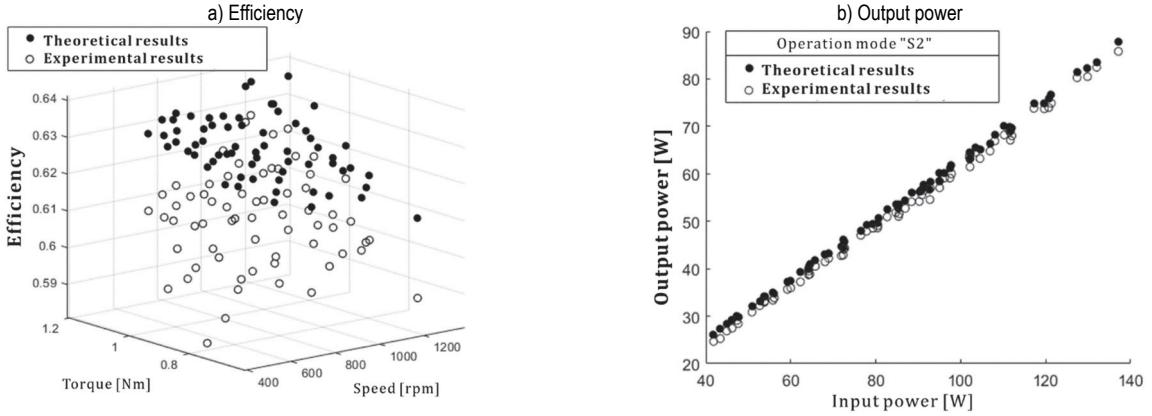

Figure 11 Theoretical and experimental results in the "*S*2" operating mode

6 CONCLUSION

When evaluating the efficiency of a constrained cycloid drive, it is necessary to consider the influence of a large number of parameters, which directly or indirectly affect the total losses of the transmission. The paper presents the expressions for determining transmission ratios, efficiency, velocities and forces acting within a constrained cycloid drive. These expressions form the basis for the development of a theoretical model for the estimation of partial and total losses of constrained cycloid drive.

The theoretical model is implemented in the software, which enables the input of various data, as well as the analysis of different variants of the simple cycloid drive. It was noticed that the biggest partial losses are those that are the result of the sliding between rollers and pins, both on the central ring and on the disc. These losses can be reduced, and therefore the overall efficiency increased, by using needle roller bearings.

In order to verify the theoretical model and software, an experimental analysis was performed. A physical model of a simple cycloid drive was created, with the basic transmission ratio i_o = 14/15. Also, a test bench was constructed and made, on which it is possible to measure input and output data in real time.

In experimental tests, with shaft *2* stopped, the efficiency varies from 61.50% to 64.85%, while the mean value is 63.49%. In the case of theoretical results, the efficiency ranges from 63.75% to 66.12%, while the mean value is 65.25%. The mean value of the additional loss factor is 1.76%. For the operation mode "*S*2", when the shaft *1* is stopped, the efficiency changes, for experimental tests, from 58.21% to 63%, while the mean value is 60.9%. In the case of theoretical results, the efficiency ranges from 61% to 63.99%, while the mean value is 62.82%. The mean value of the additional loss factor is 1.92%. Finally, a very good correlation between theoretical and experimental results can be stated. In all measurements, the mean value of the additional loss factor does not exceed 2%.

7 REFERENCES

[1] Catalogs: Sumitomo Cyclo Drive.
[2] Catalogs: Nabtesco Precision Europe GmbH.
[3] Mackic, T., Tica, M., & Suba, R. (2019). Transmission characteristics of simple cycloid drive with stepped planets. *IOP Conf. Ser.: Mater. Sci. Eng*., *659*. https://doi.org/10.1088/1757-899X/659/1/012071
[4] Malhotra, S. K. & Parameswaran, M. A. (1983). Analysis of a cycloid speed reducer. *Mechanism and Machine Theory*, *18*(6), 491-499. https://doi.org/10.1016/0094-114X(83)90066-6
[5] Kosse, V. (2007). Using hysteresis loop and torsional shock loading to assess damping and efficiency of cyclo drives. In: 14th international congress on sound and vibration (ICSV14). *Cairns, Qld*, 9-12 July 2007, 3446–3453. https://doi.org/10.1016/j.procir.2018.04.064.
[6] Gorla, C., Davoli, P., Rosa, F., Longoni, C., Chiozzi, F., Samarani, A. (2008). Theoretical and experimental analysis of a cycloidal speed reducer. *Journal of Mechanical Design*, *130*(11), 112604. https://doi.org/10.1115/1.2978342
[7] Kudryavtsev, V. N. (1966). *Planetary Transmissions reference book*. Moscow.
[8] Lehmann, M. (1984). Determination of the efficiency of cycloid cam drives. *Drive Technology*, *23*(12), United Specialist Publishers, Mainz.

[9] Chmurawa, M., John, A., & Kokot, G. (1999). The influence of numerical model on distribution of loads and stress in cycloidal planetary gear. *Proc. 4th International Scientific Colloquium Cax Techniques, Bielefeld, Germany*.

[10] Kim, K. H., Lee, C. S., & Ahn, H. J. (2009). Torsional Rigidity of a Cycloid Drive Considering Finite Bearing and Hertz Contact Stiffness. *ASME 2009 International Design Engineering Technical Conferences and Computers and Information in Engineering Conference*. https://doi.org/10.1115/DETC2009-87092

[11] Blagojevic, M., Marjanovic, N., Djordjevic, Z., Stojanovic, B., Marjanovic, V., Vujanac, R., & Disic, A. (2014). Numerical and experimental analysis of the cycloid disc stress state. *Tehnički vjesnik*, *21*(2), 377-382.

[12] Kim, K. H., Lee, C. S., & Ahn, H. J. (2009). Torsional Rigidity of a Cycloid Drive Considering Finite Bearing and Hertz Contact Stiffness. *ASME 2009 International Design Engineering Technical Conferences and Computers and Information in Engineering Conference*. https://doi.org/10.1115/DETC2009-87092

[13] Sensinger, J. W. (2010). Unified approach to cycloid drive profile, stress, and efficiency optimization. *Journal of Mechanical Design*, *132*(2), 024503. https://doi.org/10.1115/1.4000832

[14] He, H., Li, X., & Zhang, T. (2023). Multi-Tooth Contact Analysis and Tooth Profile Modification Optimization for Cycloid Drives in Industrial Robots. *Tehnički vjesnik*, *30*(1), 93-101. https://doi.org/10.17559/TV-20220403200857

[15] Ivanović, L., Josifović, D., Ilić, A., & Stojanović, B. (2011). Tribological aspect of the kinematical analysis at trochoidal gearing in contact. *Journal of the Balkan Tribological Association*, *17*(1), 37-47.

[16] Ivanović, L., Mačkić, T., & Stojanović, B. (2016). Analysis of the Instantaneous Friction Coefficient of the Trochoidal Gear Pair. *Journal of the Balkan Tribological Association*, *22*(1), 281-293.

[17] Tomović, R., Ivanović, L., Mačkić, T., Stojanović, B., & Glišović, J. (2021). Prediction of oil film thickness in trochoidal pump. *Transactions of the Canadian Society for Mechanical Engineering*, *45*(3), 374-385. https://doi.org/10.1139/tcsme-2020-0105

[18] Hussain, T., Sarangi, N., Sivaramakrishna, M., & Udaya Kumar, M. (2021). A study on the rotor profile and internal clearances of the gerotor pump used in lubricating system of gas turbine engine. *Materials Today: Proceedings*. https://doi.org/10.1016/j.matpr.2020.12.797

[19] Robison, A. J. & Vacca, A. (2021). Performance comparison of epitrochoidal, hypotrochoidal, and cycloidal gerotor gear profiles. *Mechanism and Machine Theory*, *158*, 104228. https://doi.org/10.1016/j.mechmachtheory.2020.104228

[20] Sensinger, J. (2013). Efficiency of high-sensitivity gear trains, such as cycloid drives. *ASME J Mech Des*, 135, 071006. https://doi.org/10.1115/1.4024370

[21] Salgado, D. R. & Del Castillo, J. M. (2005). Selection and Design of Planetary Gear Trains Based on Power Flow Maps. *ASME J. Mech. Des*., *127*(1), 120-134. https://doi.org/10.1115/1.1828458

[22] Blagojević, M., Kočić, M., Marjanović, N., Stojanović, B., Đorđević, Z., Ivanović, L., & Marjanović, V. (2012). Influence of the friction on the cycloidal speed reducer efficiency. *Journal of the Balkan Tribological Association*, *18*, 217- 227.

[23] Mačkić, T., Blagojević M., Babić Z., Kostić N. (2013). Influence of design parameters on cyclo drive efficiency. *Journal of the Balkan Tribological Association*, *19*, 497-507.

[24] Hsieh, C. F. (2014). Dynamics analysis of cycloidal speed reducers with pinwheel and nonpinwheel designs. *ASME J. Mech. Design*, *136*(9), 091008. https://doi.org/10.1115/1.4027850

[25] Blagojević, M., Matejić, M., & Kostić, N. (2018). Dynamic Behaviour of a Two-Stage Cycloidal Speed Reducer of a New Design Concept. *Tehnički vjesnik*, *25*(Supplement 2), 291-298. https://doi.org/10.17559/TV-20160530144431

[26] Jang, D. J., Kim, Y. C., Hong, E. P., & Kim, G. S. (2021). Geometry design and dynamic analysis of a modified cycloid reducer with epitrochoid tooth profile. *Mechanism and Machine Theory*, *164*, 104399. https://doi.org/10.1016/j.mechmachtheory.2021.104399

[27] Xu, L. & Yang, X. (2021). Relative velocity and meshing efficiency for a novel planar ball reducer. *Mechanism and Machine Theory*, *155*. https://doi.org/10.1016/j.mechmachtheory.2020.104057

[28] Tica, M., Mačkić, T., Marjanović, N., Troha, S., & Milutinovic, M. (2022). Analysis of gear ratios of two different types of cycloid drive train. *IETI Transactions on Engineering Research and Practice*., *6*(2), 18-23.

[29] Müller, H. W. (2001). Die Umlaufgetriebe; Berlin: Spinger-Verlag.

[30] Mačkić, T., Marjanović, N., Jotić, G., Tica, M., & Đurić Ž. (2021). Influence of Cycloid Disk Profile Correction on Contact Force. *15th International Conference on Accomplishments in Electrical and Mechanical Engineering and Information Technology DEMI, Banja Luka*, 2021, 28 - 29 May, 282-286.

[31] SKF, Rolling Bearings Catalogue (2014). SKF Group.

[32] Dion, J. L., Pawelski, Z., Chianca, V., Zdziennicki, Z., Peyret, N., Uszpolewicz, G., Ormezowski, J., Mitukiewicz, G., & Lelasseux, X. (2020). Theoretical and experimental study for an improved cycloid drive model. *J. Appl. Mech*. *87*, 011002. https://doi.org/10.1115/1.4044456

Contact information:

Tihomir MAČKIĆ, Research Assistant
University of Banja Luka,
Faculty of Mechanical Engineering,
Stepe Stepanović 71, 78000 Banja Luka, Bosnia and Herzegovina
E-mail: tihomir.mackic@mf.unibl.org

Nenad MARJANOVIĆ, Full Professor
University of Kragujevac,
Faculty of Engineering,
6, Sestre Janjic Str., 34000 Kragujevac, Serbia
E-mail: nesam@kg.ac.rs

Milan TICA, Associate Professor
(Corresponding author)
University of Banja Luka,
Faculty of Mechanical Engineering,
Stepe Stepanović 71, 78000 Banja Luka, Bosnia and Herzegovina
E-mail: milan.tica@mf.unibl.org

Sanjin TROHA
University of Rijeka,
Faculty of Engineering,
Vukovarska 58, 51000 Rijeka, Croatia
E-mail: sanjin.troha@riteh.hr

Miroslav MILUTINOVIĆ, Associate Professor
University of East Sarajevo,
Faculty of Mechanical Engineering,
Vuka Karadžića 30, 71123 East Sarajevo, Bosnia and Herzegovina
Email: miroslav.milutinovic@ues.rs.ba

Nebojša RAŠOVIĆ, Associate Professor
University of Mostar,
Faculty of Mechanical Engineering, Computing and Electrical Engineering,
Matice hrvatske b.b, 88000 Mostar, Bosnia and Herzegovina
Email: nebojsa.rasovic@fsre.sum.ba